Silicon (2021) 13:2445–2459
https://doi.org/10.1007/s12633-020-00588-x

ORIGINAL PAPER

Application of Environmentally-friendly Cooling/Lubrication Strategies for Turning Magnesium/SiC MMCs

Navneet Khanna[1] · Prassan Shah[1] · Narendra Mohan Suri[2] · Chetan Agrawal[1] · Sandeep K. Khatkar[3] · Franci Pusavec[4] · Murat Sarikaya[5]

Received: 14 April 2020 / Accepted: 3 July 2020 / Published online: 19 July 2020

Abstract

The material having high strength to weight ratio is constantly in high demand for automotive industries to increase fuel efficiency. With this view, AZ91/5SiC (an Mg-based Particulate Metal Matrix Composites (PMMCs)) is fabricated using an in-house developed stir casting setup and characterized through Field Emission Scanning Electron Microscopy (FESEM) with Energy-Dispersive X-ray Spectroscopy (EDS) analysis. However, the machinability of PMMCs is found to be lower due to the existence of harder ceramic constituents and appropriate cutting fluid strategies are required to follow to combat this situation. But limited studies are available identifying the impact of recently developed sustainable cooling and lubrication techniques on machining performance when PMMCs is turned. To fill this bridge, customized setups of minimum quantity lubrication (MQL), cryogenic and CryoMQL machining with LN_2 have been developed to provide eco-friendly cutting fluid approaches to turn AZ91/5SiC. The cutting force, energy consumption, surface roughness (R_a) and chip breakability index (C_{in}) have been analyzed for MQL, cryogenic and CryoMQL techniques with variation in process parameters. By considering the average value of all turning tests, 64.65% and 40.39%; and 11.49% and 7.13% higher value of cutting force and energy consumption is found correspondingly for cryogenic and CryoMQL machining respectively as compared to MQL technique respectively. Overall, 25.59% and 18.35% lower values of R_a have been observed for CryoMQL technique as compared with MQL and cryogenic machining respectively. The powder type chips with comparable higher values of C_{in} have been found in all three cooling and lubrication techniques.

Keywords Magnesium AZ91/5SiC PMMCs · SiC · Cryogenic machining · MQL · CryoMQL machining

Nomenclature

MQL	Minimum quantity lubrication
PMMCs	Particulate metal matrix composites
R_a	Average surface roughness in μm
C_{in}	Chip breakability index
LN_2	Liquid nitrogen

✉ Prassan Shah
prassan.shah.17pm@iitram.ac.in

Navneet Khanna
navneetkhanna@iitram.ac.in

Narendra Mohan Suri
nmsuri65@yahoo.com

Chetan Agrawal
chetanagrawal@iitram.ac.in

Sandeep K. Khatkar
sandeepkhatkar99@gmail.com

Franci Pusavec
Franci.Pusavec@fs.uni-lj.si

Murat Sarikaya
msarikaya@sinop.edu.tr

1 Advanced Manufacturing Laboratory, Institute of Infrastructure Technology Research and Management (IITRAM), Ahmedabad 380026, India

2 Department of Production and Industrial Engineering, Punjab Engineering College, Chandigarh 160012, India

3 Department of Mechanical Engineering, Chandigarh Engineering College, Mohali 140307, India

4 Faculty of Mechanical Engineering, University of Ljubljana, Askerceva 6, 1000 Ljubljana, SI, Slovenia

5 Department of Mechanical Engineering, Sinop University, 57030 Sinop, Turkey

LCO_2	Liquid carbon dioxide
CryoMQL	Hybrid machining which combines cryogenic and MQL machining
FESEM	Field emission scanning electron microscope
f	Feed rate (mm/rev) in longitudinal direction
EDS	Energy-dispersive X-ray spectroscopy
v_c	Cutting speed in m/min
r_ε	Cutting tool nose radius in mm
CGM	Chip grade matrix
BUE	Built-up edge

1 Introduction

The composites are increasingly replacing conventional homogenous materials due to their superior properties like high stiffness, high specific strength, low thermal expansion and superior wear resistance. Particularly, Mg-based AZ91 PMMCs is extensively used in auto and aero-industries due to their better creep resistance, fatigue strength, and ultimate tensile strength at elevated temperature [1–5]. To use these materials as a moving member in the machine, it is required to perform finishing operation. Turning process is the most commonly used finishing operation for cylindrical shaped components. PMMCs is highly anisotropic in nature as compared to conventional metallic materials and tough to machine due to the existence of hard ceramic particles within a softer matrix of metal material [6]. To improve the machinability of PMMCs, industries are using different cooling and lubrication techniques to reduce cutting zone temperature and friction between tool and workpiece that directly affect machining performance [7].

The cost of coolant and lubricant composes approximately 17% of production cost in machining operations. The usage of conventional cutting fluid also creates a hazard to worker's health and requires extra chip recycle facility before dumping of chips into the environment [8, 9]. This fact leads to develop sustainable cooling and lubrication technologies in machining processes that can reduce the cost of production without harming the environment, worker's health, and quality of machined parts. In this context, advanced manufacturing laboratory (IITRAM) and its collaborators are constantly evolving sustainable cutting fluid strategies to provide eco-friendly alternatives for cutting difficult to machine materials [10–13].

In MQL application, a minute quantity of cutting fluid (10–200 ml) with pressurized air is consumed per hour in comparison to thousands of milliliters of cutting fluid consumption for conventional flood machining. Due to a minimal amount of cutting fluid consumption, MQL technique eliminates the chip recycle process. These pressurized mist particles have higher reachability into the cutting zone, especially for closed face machining operations like drilling and turning [14–16]. In cryogenic machining, low-temperature cryogenic fluid is used in place of harmful cooling and lubrication techniques containing petroleum-based additives. Generally, LN_2 and LCO_2 are used as cryogenic fluids in cryogenic machining due to their inert nature and availability at low-cost. The LN_2 quickly dissipates heat from the cutting zone by converting into vapor due to its low boiling point (−195.8 °C) as compared to LCO_2 (−78.5 °C). It does not react with tool and workpiece material due to its inert nature. It is ecological and environment-friendly because it does not leave any marks on chips. However, proper safety is required while handling LN_2 as it can cause a cold burn if it comes in direct contact with the skin [17, 18].

Recently, Khanna et al. [19] compared LCO_2 and LN_2 as cutting fluids with dry condition based on machining performance and sustainability aspects for turning AXZ911/10SiC. The lower cutting force and power requirement were observed for LN_2 as cutting fluid while better results of surface roughness and sustainability indicators were found for dry machining. Yin et al. [20] formed an analytical model to predict the machined surface temperature of PMMCs viz. Al 2024/SiC and validated experimentally for orthogonal turning operation. The model was found quite accurate with a maximum 16% error between analytical and experimental results of temperature. Soorya Prakash et al. [21] analyzed the effect of particle size, weight percent of reinforcement, v_c, f and depth of cut on surface roughness and material removal rate for turning Al6061 T6/rock dust MMCs. The f was found to be a significant parameter affecting surface roughness following v_c and weight percent of rock dust respectively in decreasing order. Tamizharasan et al. [4] compared the chip thickness ratio for several combinations of v_c, f and depth of cut when Al-Cu/SiC MMCs was turned. It was observed lower chip thickness ratio at higher value of v_c with lower value of f and depth of cut.

Besides, previous studies related to the current research area (especially on the machining of Mg-based alloys and the environmentally friendly cooling/lubrication strategies used in this study) are presented. Accordingly, it was reported that the better results of R_a and C_{in} were found when ultrasonic assisted turning (UAT) was employed to turn AZ91/5SiC. A further improvement of 36.50% and 15% for surface finish and chip breakability respectively were seen when UAT was integrated with cryogenic machining with LN_2 [22]. The larger value of compressive stress (100 MPa) was found as compared to dry machining when Mg-based AZ31B-O was turned [23]. It was observed

Table 1 Chemical composition of AZ91 magnesium alloy in wt.%

Element	Mg	Zn	Al	Mn	Si	Trace elements (Fe, Cu, Ni and Sn)
Percentage	90.75	0.775	8.40	0.03	0.034	0.008

Table 2 Details of reinforcement

Reinforcement	Size	Density
Silicon Carbide	67 μm	3.21 g/cm^3

better results in terms of reduced cutting zone temperature, lesser tool wear and surface topography when Al/SiC PMMCs was turned by ultrasonic-assisted MQL turning [24]. The parallel texture on the cutting tool provided better results of cutting force, microhardness and friction coefficient when Mg-based ZK60 alloy was turned with LN_2 as cutting fluid in comparison with dry machining [25].

Apart from MQL, cryogenic and UAT machining of Mg-based alloys and PMMCs, CryoMQL machining was compared with dry, MQL and cryogenic machining for Ti-based alloys, superalloys, and difficult-to-cut steel alloys. It has been observed approximately 54% reduction in tool wear for machining 3Cr2NiMo steel when UAT and nano-fluid were accompanied with CryoMQL as compared to conventional CryoMQL [26]. It was found a decrement in surface roughness and thickness of deformed grains layer by 29% and 15% respectively under CryoMQL, in contrast with dry machining for turning Ti-6Al-4 V [27]. The lesser values of cutting force were found for turning Ti-6Al-4 V with LN_2 as cutting fluid in comparison with CryoMQL and flood machining, correspondingly in decreasing order [28]. The better results in terms of machining performance were found for CryoMQL with LCO_2 while comparable better results of life cycle assessment were found for CryoMQL with LN_2 and LCO_2 as compared to dry, wet, MQL, and cryogenic fluids with LCO_2 and LN_2 for turning AISI 304 steel [29]. A similar kind of better results for machining performances were also observed for CryoMQL machining in comparison with MQL and LN_2 as cryogenic fluid when Inconel 625 was turned [30].

Though a comparison of MQL, cryogenic and CryoMQL machining has been found in previous studies for many difficult-to-cut materials, machining performance of AZ91/5SiC is not investigated in depth more specifically

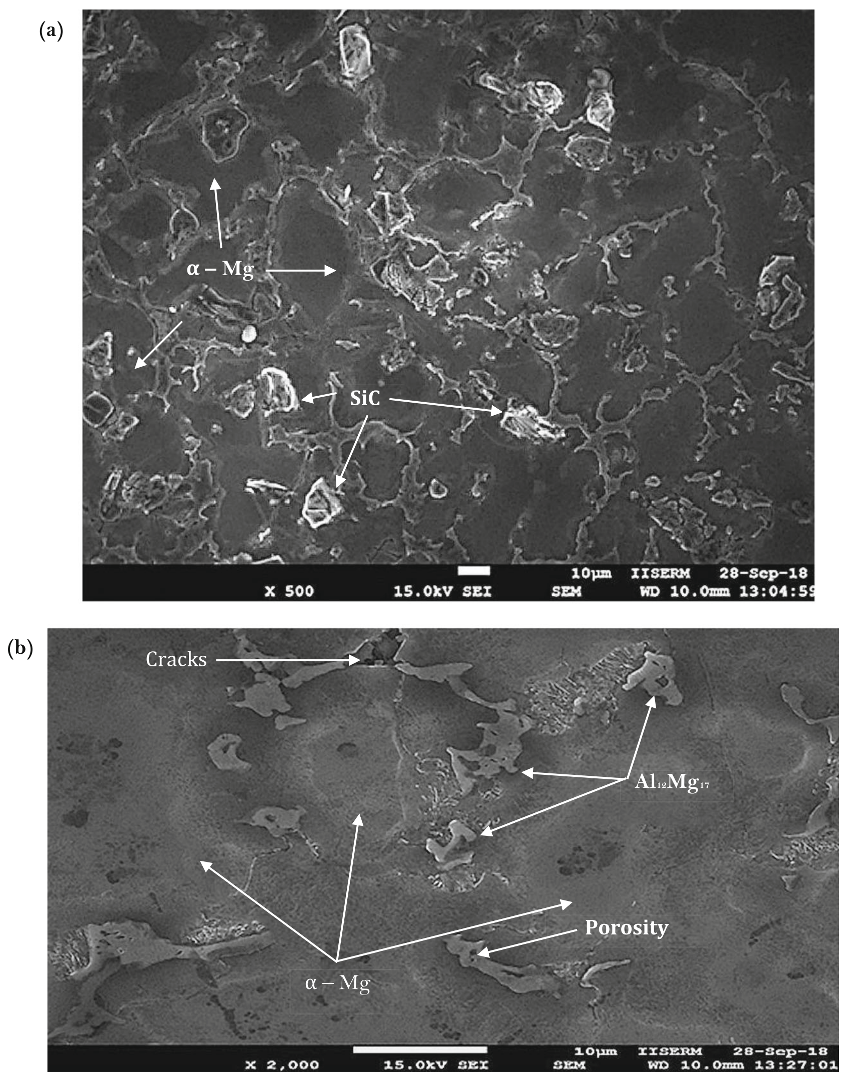

Fig. 1 SEM image of Mg-based AZ91/5SiC PMMCs at **(a)** 500 X and **(b)** 2000X magnification

when above sustainable cooling and lubrication techniques are employed. In this context, this comprehensive study beginning from fabrication to machining signifies a contribution to not only researchers and academia but also industrialists.

This paper is organized into four sections. The second section describes an experimental setup used to fabricate PMMCs material and research methodology employed for this investigation. The second section has two subsections; in the first subsection, details of in-house developed Mg-based AZ91/5SiC PMMCs material are presented. While in the second subsection, experimental setups, design of experiments and machinability tests with measurement methods followed for this study are described. The third section presents the results and discussion based on experimentation. The influence of cutting conditions on responses namely cutting force, energy consumption, R_a and C_{in}, are discussed in consecutive subsections of section three. Finally, the conclusions on the basis of discussion on results are presented in section four.

2 Material and Methods

2.1 In-House Casting Process to Fabricate AZ91/5SiC PMMCs

The Mg-based metal matrix composites (AZ91/5SiC PMMCs) was fabricated by vacuum stir casting setup. The Mg, Al, and Zn were added to furnace, which was heated up to 800 °C in an environment of SF_6 and argon gas in the ratio of 1:4. After melting of metals, the stirrer was allowed to rotate at 300 rpm to blend all molten metal. Subsequently, preheated reinforcement particles (5% wt. SiC) at 300 °C were added in a furnace and stirred thoroughly. The molten metal was poured into the preheated die at 150 °C. Table 1 and Table 2 describe the elemental composition of fabricated alloy (AZ91) and details of SiC reinforcement, respectively.

2.1.1 Microstructure Analysis of AZ91/5SiC Composites

The FESEM images of the fabricated composites at magnification of 500 X and 2000X are presented in Fig. 1 (a) and (b) respectively. The α- phases (Mg) and β- phases ($Al_{12}Mg_{17}$) were found along the grain boundaries in fabricated Mg-based AZ91/5SiC PMMCs.

It is observed the grey regions exhibited α phases, which are surrounded by a white region, i.e., β- phases ($Al_{12}Mg_{17}$). Reinforced SiC particles are not spotted in higher magnification of FESEM images. However, reinforcement particles in fabricated MMCs are visible with lower magnification (500 X), as shown in Fig. 1 (a). The distribution of ceramic particles and interfacial bonding between metal matrix and reinforced particles affect mechanical properties viz. hardness, rupture strength, ductility [31]. From Fig. 1(a) and (b), quite uniform distribution with a little agglomeration of reinforced particles and interfacial surfaces of SiC particles can be observed within the metal matrix of AZ91 alloy. However, a small number of voids and cracks can also be observed in FESEM images. Typical EDS (Energy-dispersive X-ray spectroscopy) profiles of AZ91/5SiC at different positions (indicated with a pink rectangle) reveal the clear peaks of Mg, Al, Zn, and C as described in Fig. 2.

2.2 Experimental Details for Machining Experiments

Four subsections are discussed in this section. The MQL setup used in this study has been discussed in the first subsection. The second subsection discusses cryogenic and CryoMQL machining setup. The design of experiments is discussed in the third subsection while details of machinability tests with measurement methods are presented in fourth subsection of this section.

2.2.1 Experimental Setup of MQL Machining

It has been reported that the efficiency of MQL technique depends on delivery system parameters like air pressure, angle between nozzle and horizontal axis, standoff distance (distance between nozzle and substrate), and flow rate of oil. It has been also noticed that higher air pressure can form a mist of oil efficiently [14]. In this view, as per the maximum capacity of used compressor, 5 bar pressure is selected. A similar methodology described by Setti et al. [9] has been used to

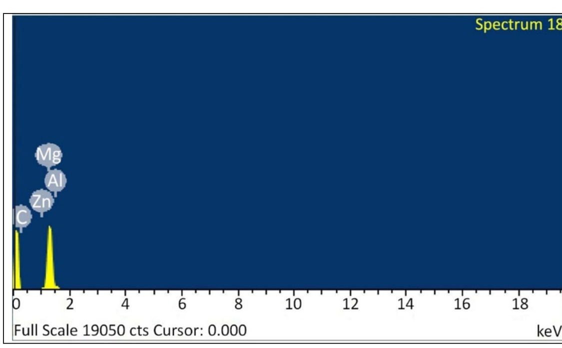

Element	Weight %	Atomic %
C K	6.98	13.27
O K	3.44	4.91
Mg K	76.64	71.89
Al K	10.94	9.24
Zn L	2.00	0.70
Total	100.00	

Fig. 2 EDS analysis of fabricated Mg-based AZ91/5SiC PMMCs

Table 3 The values of force for different combinations of standoff distance and nozzle angle

Distance (mm)	Angle				
	15°	30°	45°	60°	75°
30	25.63 (N)	23.20 (N)	21.36 (N)	19.53 (N)	39.72 (N)
50	11.59 (N)	22.58 (N)	21.97 (N)	16.47 (N)	18.92 (N)
70	12.20 (N)	25.02 (N)	28.68 (N)	14.64 (N)	22.58 (N)
90	28.68 (N)	18.31 (N)	23.19 (N)	20.75 (N)	25.63 (N)
110	18.31(N)	17.70 (N)	27.46 (N)	17.08(N)	38.40 (N)

optimize MQL parameters namely nozzle angle, standoff distance, and flow rate.

To optimize the standoff distance and the angle between nozzle and substrate, force exerted on dynamometer is measured when a spray of mist is applied to it. Table 3 presents different combinations of nozzle angle and standoff distance for which the values of force are measured. The values of standoff distance and angle between nozzle and horizontal axis is varied from 30 to 110 mm in an interval of 20 mm and 15° to 75° in an interval of 15° respectively. As per the results of cutting force, it is concluded that when nozzle angle is 75° and standoff distance is 30 mm, it generates a maximum force on the substrate.

The flow rate of cutting oil was varied up to 30 ml/h when cast Mg alloy was machined with MQL [32]. In this context, a flow rate of oil in MQL is varied from 2 to 20 ml/h in an interval of 3 ml/h to identify an optimum flow rate for turning AZ91/5SiC PMMCs. The droplet quality is measured in terms of a number of droplets, average size and percentage of surface area covered by droplets. To measure droplet quality, droplets of oil are collected on the silicon wafer, as illustrated in Fig. 3 at different flow rate, as shown in Table 4. The images of droplets are analyzed by open-source Image J software as presented in Fig. 3.

The ester-based polyol synthetic cutting oil gives superior results of increased tapping energy efficiency, storage stability, oxidation stability and biodegradability for MQL machining [33]. With this view, neat synthetic oil was used to perform MQL machining. The elemental composition of cutting oil is mentioned in Table 5 along with a summary of optimized MQL parameters used for MQL machining.

2.2.2 Experimental Setup of Cryogenic and CryoMQL Machining

An indigenously developed LN_2 cryogenic delivery setup has been used in this study. The primary components of this LN_2 delivery setup are spray nozzle, LN_2 cylinder, and vacuum jacketed hose. LN_2 has been stored at 6 bar in LN_2 cylinder (Dewar), which is equipped with LN_2 level indicator and valves for safety, flow control and venting. The self-patented phase separator has been used to deliver LN_2 in cutting zone [34]. In cryogenic machining, a nozzle having a 2 mm diameter has been used to form the jet of LN_2 at rake face.

To perform CryoMQL machining, setup of MQL and cryogenic machining are merged, as illustrated in Fig. 4. In the CryoMQL machining setup, LN_2 is supplied at a rake face while MQL is supplied at flank face of cutting insert.

Fig. 3 An illustration of a procedure to measure droplet quality

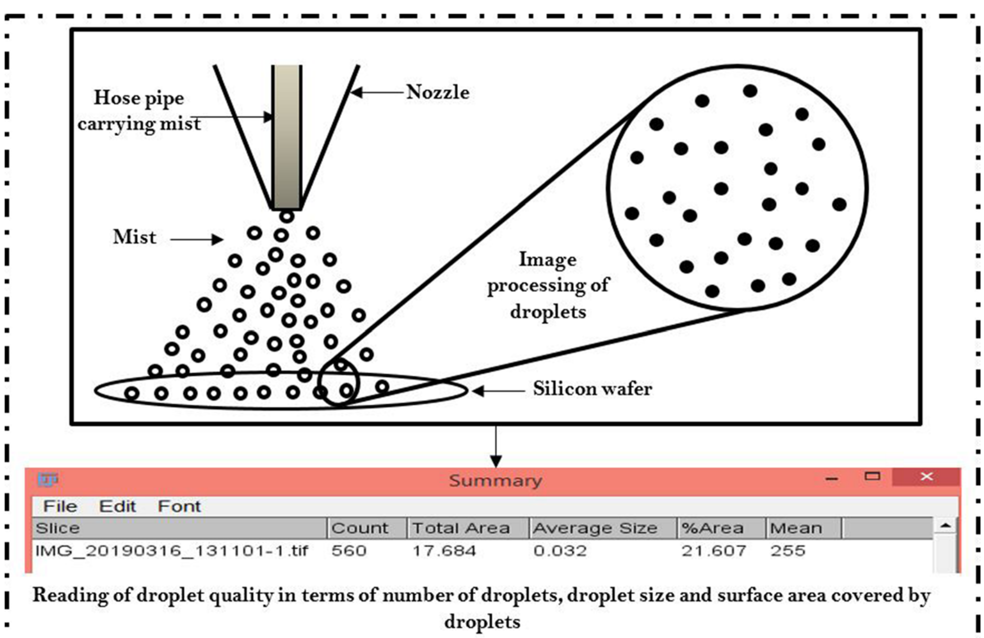

Table 4 Results of droplet quality for different flow rate

Sr No.	Number of droplets	The flow rate in ml/h	Average size of droplets in mm	% of area covered by droplets
1	191	2	0.044	10.331
2	224	5	0.047	12.169
3	1030	8	0.005	5.74
4	291	11	0.025	9.51
5	951	14	0.022	27.918
6	560	17	0.032	21.607
7	208	20	0.108	24.689

2.2.3 Design of Experiments (DoE)

A rigid semiautomatic lathe has been employed to perform all turning tests as shown in Fig. 5. Each experiment is replicated two times with unused cutting edge to lower the effect of experimental noise on responses. By considering improved machining performance of non-hydrogenated diamond-like carbon (DLC) coating for machining AZ91 alloy [35], in this study, Kyocera made hydrogen-free CNMG120404AH PDL025 inserts having DLC coating were used with MCLNR 2020 K12 tool holder. The summary of machining conditions along with ISO specification of a cutting tool is presented in Table 6. The material (AZ91/5SiC) used for turning tests was a cylindrical rod having a diameter of 20 mm and 190 mm length. It has been observed that DoE plays a vital role in improving the efficiency of machining process [36]. In this study, experiments are planned as per the full factorial design. Three levels of each, v_c (v_{c1} = 62 m/min, v_{c2} = 41 m/min, v_{c3} = 27 m/min), f (f_1 = 0.111 mm/rev, f_2 = 0.222 mm/rev, f_3 = 0.333 mm/rev), and cutting fluid strategy (MQL, cryogenic, and CryoMQL) are selected to analyze the effect of cutting conditions when Mg-based AZ91/5SiC PMMCs is turned. The value of depth of cut is kept as 0.5 mm constant for all experiments.

2.2.4 Machinability Tests with Measurement Methods

To investigate the effect of different cutting conditions viz. MQL, Cryogenic and CryoMQL with variation in turning process parameters, cutting force, energy consumption, R_a and C_{in} have been measured.

The cutting force generated during machining is highly influenced by factors such as workpiece material, machining parameters, friction at tool-chip contact, and cutting fluid strategies [37]. The result of cutting force reflects tool wear, vibration generated and power consumption during machining. In this view, the influence of cutting force for three various cooling and lubrication techniques have been measured. Kistler made 4-component 9272 A type tool dynamometer has been used to attain the data of cutting force. The working of dynamometer with its components is shown in Fig. 5. The piezoelectric rings fixed on dynamometer produce the charge as per the value of force applied on it. This generated charge is transferred from the rings to multi charge amplifier through highly insulated cable. This charge is converted into the signals of voltage by a multichannel charge amplifier (Type 5080 A). These voltage signals received from the charge amplifier are processed and converted into digital form by data acquisition system

Table 5 List of MQL parameters

MQL parameters	Values
Cutting oil	Main constituent: - Pentaerythritol tetra oleate. Chemical formula: - $C_{77}H_{140}O_8$ (92%), Other constituents: - Zinc Dialkyl Di Thiophosphate (5%) and Antioxidant (3%), Kinematic viscosity: 70 cSt at 40 ° C, Specific gravity: 0.92 at 20 °C and Flashpoint: 210 °C
Standoff distance	30 mm
Air pressure	5 bar
Nozzle angle	75°
Nozzle diameter	2 mm
Flow rate of oil	14 ml/h

(Type 5697 A). Finally, these digital signals in the form of force are displayed and stored by Dyanoware software (Type 2825A) equipped with computer interface. To have an accurate reading, the dynamometer has been calibrated keeping the sensitivity of piezoelectric rings as 7.6 pC/N in X and Y directions while −3.6 pC/N in the Z direction. To have an accurate measurement of cutting force, 1000 readings have been taken per second.

It is found that the requirement of electrical energy increases every year at a rate of 1.5% from 2007 to 2030. The manufacturing sector consumes 30% of the total electricity produced in the World [38] . So, the machining process being

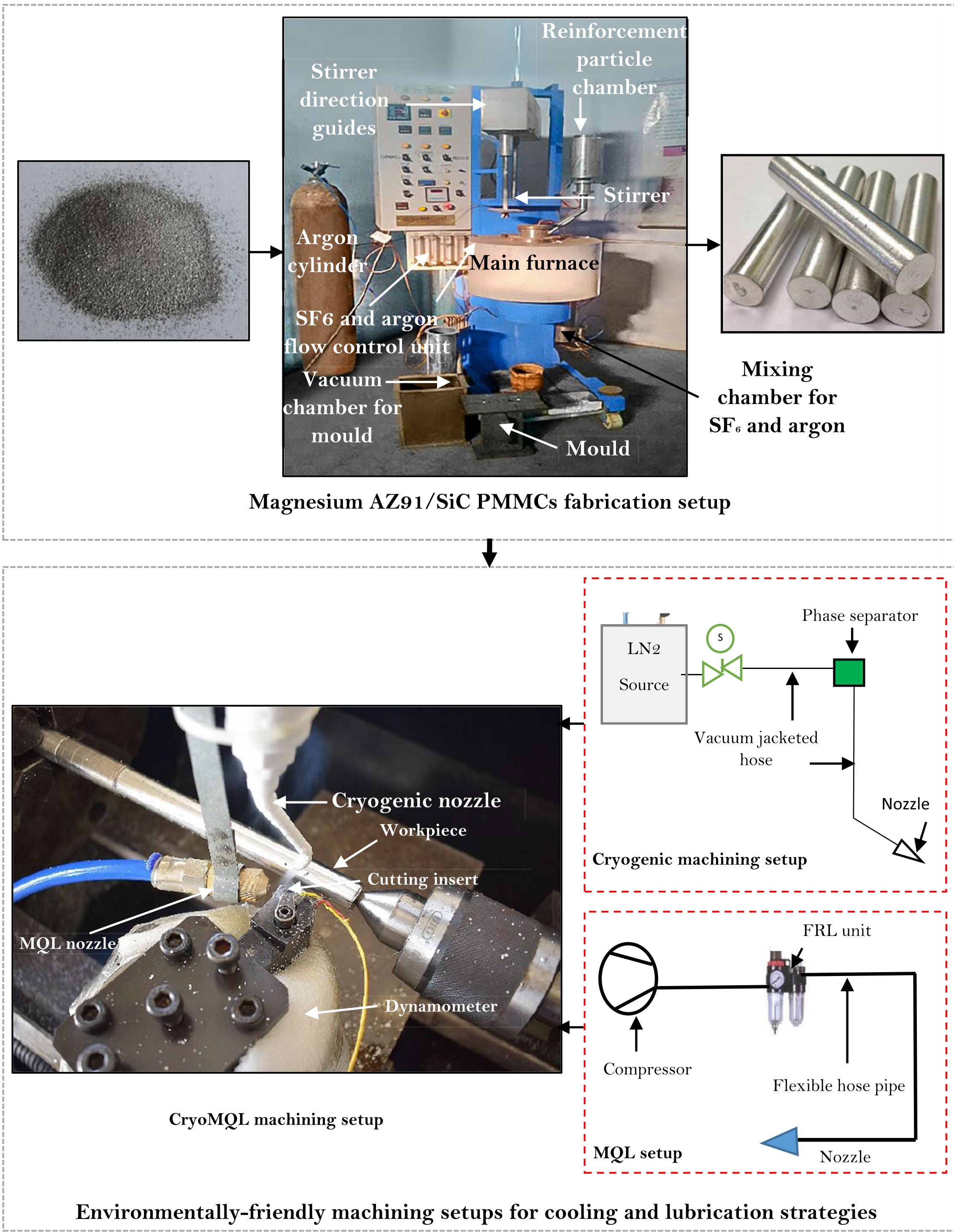

Fig. 4 Experimental setup for stir casting and machining processes

a part of manufacturing sector has high potential to reduce energy consumption. With this view, to identify the impact of energy consumption on process parameters and cutting conditions, Fluke made power quality and energy analyzer (435 Series II) has been used to measure energy consumed during machining as shown in Fig. 6. The four Bayonet Neill Concelman (BNC) plugs have been connected to measure the current while four banana-type clamps are connected to evaluate the voltage drawn by the lathe machine.

The data of surface roughness is essential in the context of corrosion resistance, fatigue strength and dimensional accuracy specifically when the parts are required to assemble. In this context, surface roughness in term of R_a has been measured for different cutting fluid strategies and turning process parameters by Surtronic S128 (product of Taylor and Hobson) contact-type surface roughness tester as shown in Fig. 7. The evaluation length, cut-off length and sampling length have been kept as 4.0 mm, 0.8 mm and 0.8 mm correspondingly as per ISO 4288:1996 [39]. For every turning test, five readings of R_a have been taken at various locations of machined surface.

3 Results and Discussion

The three cooling and lubrication techniques of machining namely MQL, cryogenic and CryoMQL are compared and analyzed based on the values of responses i.e., cutting force, energy consumption, R_a and C_{in} at different process parameters in the following subsections.

3.1 Cutting Force

Figure 8 presents comparison of cutting force with a change in process parameters and cutting conditions. It is observed higher cutting force in cryogenic machining followed by CryoMQL and MQL machining in succession. By considering the average value of all turning tests, 40.39% and 64.65% higher cutting force are observed for CryoMQL and cryogenic fluid with LN_2 respectively in comparison with MQL technique. The lower cutting force found for MQL technique is because of effective lubrication at the tool-chip interface. It has been found that the adsorption of oil particles can be done

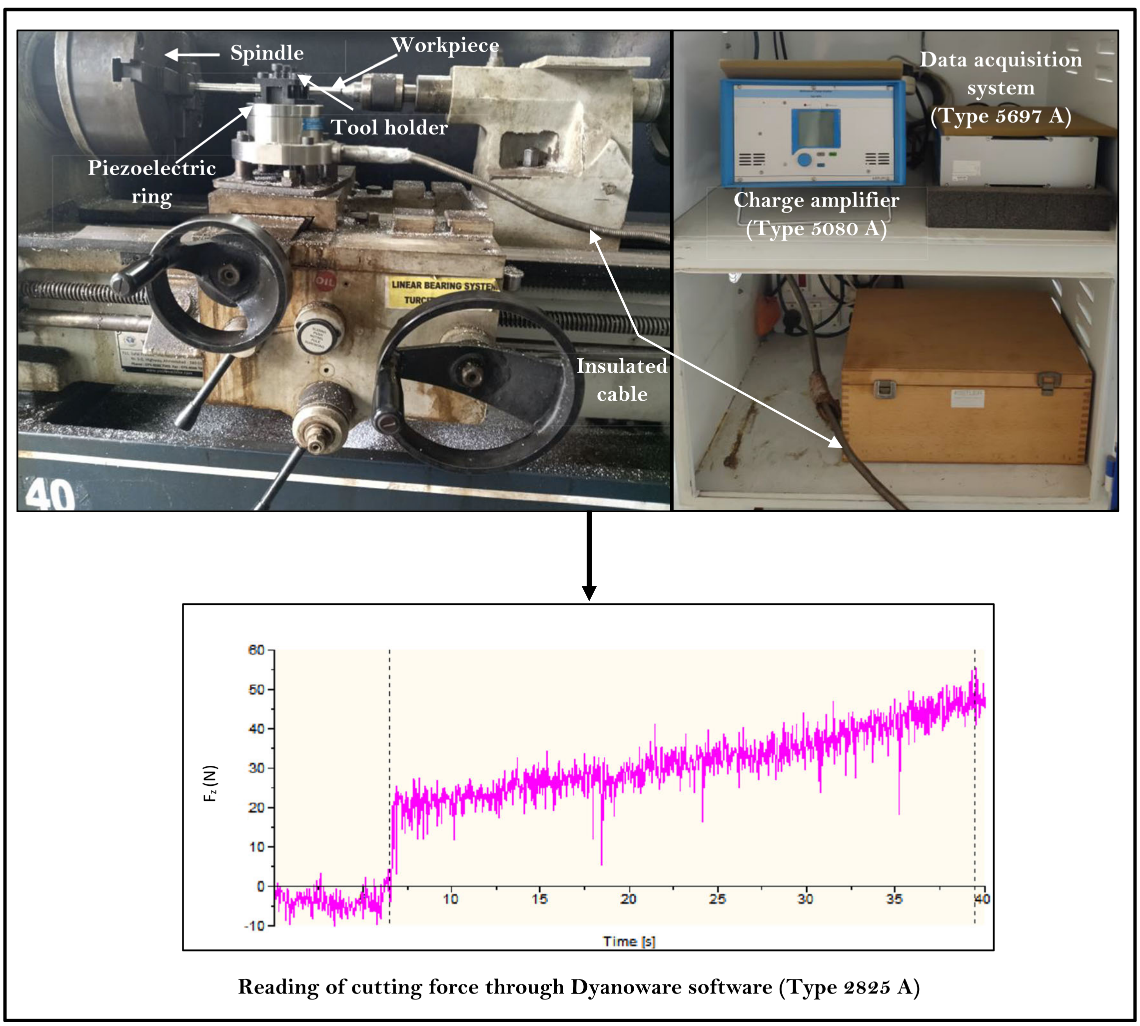

Fig. 5 An image for setup and components of dynamometer to measure cutting force

Table 6 Details of machining conditions

Parameter	Description
Workpiece material	AZ91/5SiC (ø = 20 mm, 190 mm length)
Tool holder	MCLNR 2020 K12 (as per ISO specification)
Insert and working tool geometry	Uncoated Kyocera made CNMG120404AH PDL025 inserts
	Orthogonal rake angle = −6° inclination angle = −6 °, clearance angle = 6°
	Primary cutting-edge angle (ψ) = 95° nose radius (r_ε) = 0.4 mm, insert thickness = 4.76 mm, size of insert describing the diameter of inscribed circle = 12.7 mm
Depth of cut (mm)	0.5
V_c (m/min)	62, 41 and 27
f (mm/rev)	0.111, 0.222 and 0.333
Cutting condition	MQL, Cryogenic and CryoMQL machining with LN_2

effectively on tool if mist lubrication is used as in MQL technique. Figure 9 shows the basic difference between conventional flood and MQL techniques in terms of contact of cutting oil with a tool. Besides, the presence of oxygen in pressurized air produces metallic oxide and cutting oil makes soap like boundary lubrication quickly with metallic oxide as compared to metallic surface [40]. It lowers the friction between tool-chip interface and eventually reduction in cutting force is observed. A similar kind of observation has been seen when mist lubrication is provided considering oxygen as a gaseous medium [41, 42]. But in cryogenic and CryoMQL machining, strain hardening caused due to lower temperature increases the cutting force in comparison to MQL machining [37]. In CryoMQL machining, reduced cutting force is found in comparison with cryogenic machining because of an application of extra lubricant at a flank face which reduces friction and lowers cutting force.

At a lower value of f (0.111 mm/rev), cutting force decreases as the value of v_c increases for cryogenic and CryoMQL techniques at most of the tests. The opposite trend is found for MQL technique wherein an increment in value of v_c raises cutting force. The cutting zone temperature is raised when the value of v_c is increased. This situation becomes more predominant in case of MQL technique where there is no provision of coolant. This higher temperature generated in the cutting zone raises diffusion wear specifically for MMCs like AZ91/5SiC [43]. Besides, the softening of PMMCs at higher temperature pulls out hard ceramic particles easily from metal matrix which exerts a higher force on cutting tool. So, as the value of v_c increases, cutting force raises in MQL machining. Extremely lower temperature observed in cryogenic and CryoMQL machining lowers diffusion wear and maintains the integrity of SiC particles within metal matrix. However, reduction in workpiece hardness at a higher value of v_c due to a rise in temperature decreases cutting force for cryogenic and CryoMQL machining [43]. But, at intermediate (0.222 mm/rev) and higher (0.333 mm/rev) value of f, opposite trend is observed for values of cutting force in comparison with lower value of f. As the value of v_c decreases with a higher value of f, intermittent contact of hard reinforced particles increases with cutting tool. It attributes a higher cutting force at a lower value of v_c and higher value of f in MQL machining. However, in case of cryogenic and CryoMQL machining, intermittent action of hard particles does not signify to rise cutting force due to the overall embrittlement of workpiece material.

3.2 Energy Consumption

Figure 10 compares the value of energy consumption with a change in v_c and f for all three cutting conditions. The values of energy consumption are higher for CryoMQL and cryogenic machining in comparison with MQL machining for most of the turning tests. A comparable trend was also found for the results of cutting force. By considering the mean of all turning tests, 11.49% and 7.13% higher value of energy consumption is found for cryogenic and CryoMQL machining in comparison with MQL technique respectively. In literature also, it is reported that power consumption increases up to 1.5% with cryogenic LN_2, in contrast to dry machining due to increased hardness of workpiece [18]. However, at higher cutting

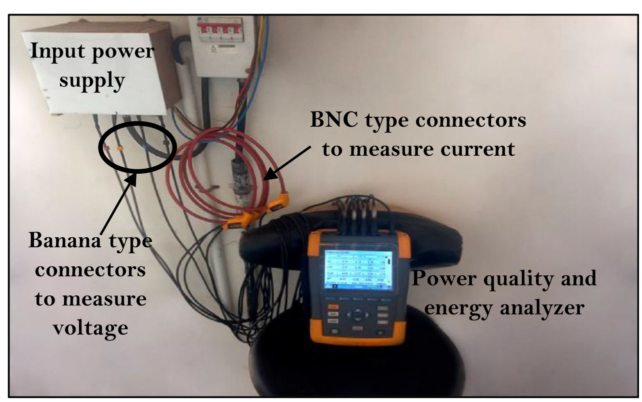

Fig. 6 An image for the setup of power quality and energy analyzer to measure energy consumption

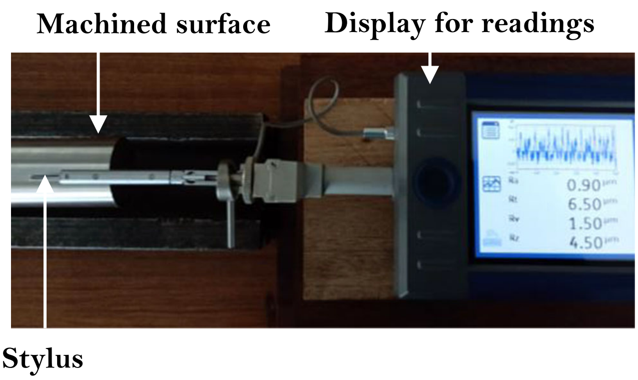

Fig. 7 An image for the setup of surface roughness measurement

parameters ($v_{c1}f_3$), energy consumption is almost comparable for all three cutting conditions. Hence it is beneficial to use cryogenic and CryoMQL machining at higher levels of cutting parameters without a significant increment in energy consumption.

As observed from Fig. 10, energy consumption decreases for all three cutting conditions at all values of v_c when value of f raises. This is due to a reduction in machining time with increment in the value of f. As the value of v_c increases, energy consumption raises at lower and intermediate values of f for most of the cooling and lubrication techniques. This is due to an increment of spindle rotation which increases requirement of power and hence energy consumption as shown in Eq. 1.

$$P = \frac{2\pi NT}{6000} \quad (1)$$

Here P denotes power consumed by machine in kW, while T and N denote torque required to rotate spindle and revolution of spindle per minute, respectively. At a higher value of f, energy consumption rises as the value of v_c decreases irrespective of cutting condition. It is attributed to increased vibration at a combination of lower value of v_c and higher value of f [44].

3.3 Surface Roughness

The value of R_a has been compared at various values of turning process parameters and cutting fluid strategies through Fig. 11.

The 25.59% and 18.35% lower values of R_a have been observed in case of CryoMQL machining considering all turning tests, in comparison with MQL and LN_2 as cryogenic fluid respectively. As discussed previously, the higher cutting zone temperature found for MQL technique weakens the matrix integrity. The pull out of SiC particles at higher temperature forms BUE on cutting edge and lowers the surface roughness as found for MQL machining. The decrement of hard SiC particles' influence was observed in deteriorating surface finish under cryogenic and CryoMQL machining techniques. At cryogenic temperature, the hardness of matrix material raises, and PMMCs behaves more like homogeneous material [45]. Apart from it, an improved surface finish observed under cryogenic and CryoMQL machining is due to the capability of LN_2 to extract heat quickly from cutting zone, as shown in Fig. 12. As per Fig. 12, higher normal stress is generated

Fig. 8 Variation in cutting force at different v_c and f under various cutting fluid strategies

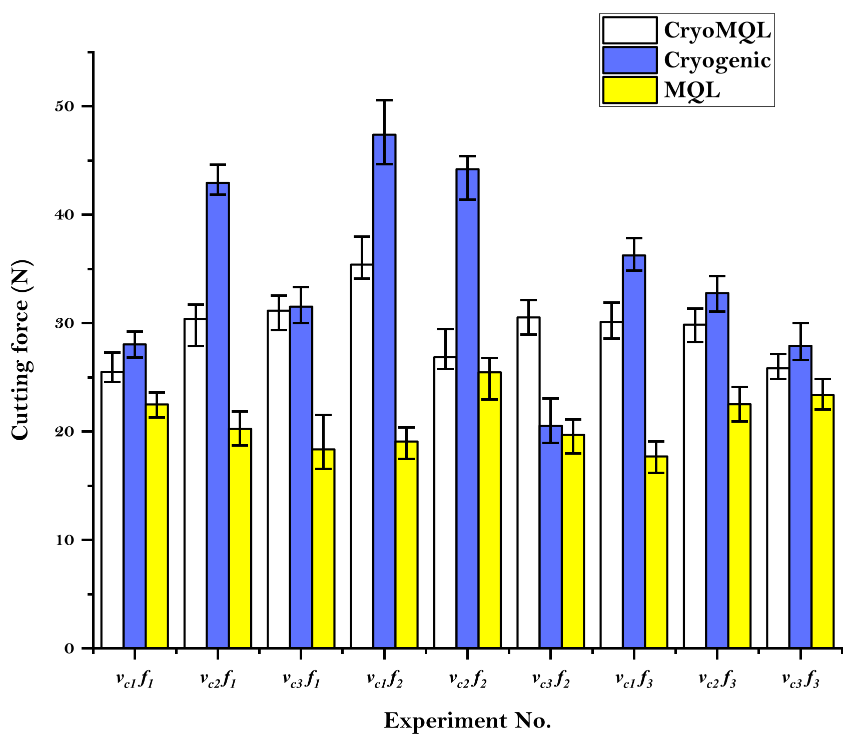

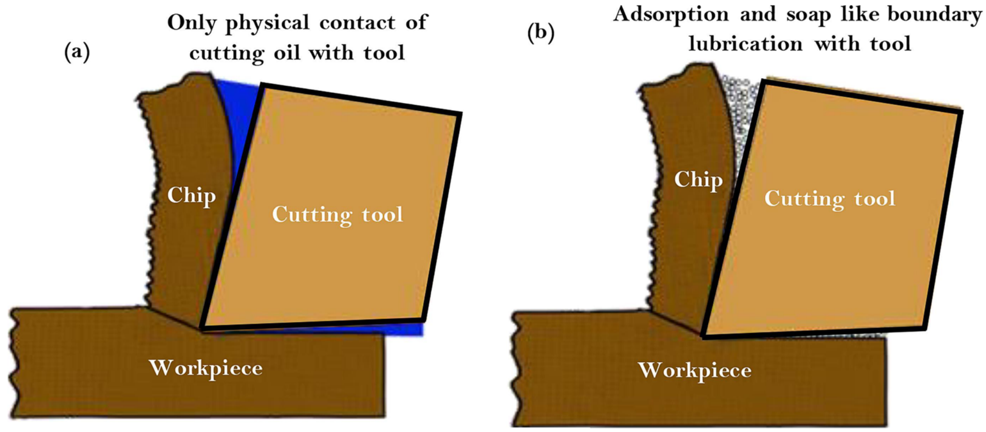

Fig. 9 A schematic to present contact of cutting oil with a tool for **(a)** Flood cooling and **(b)** MQL machining [41]

between tool and chip at the secondary shear zone. This is a cause of high temperature generation which increases adhesion of chip on the tool and hence BUE formation. The supply of pressurized LN_2 at rake face effectively reduces adhesion of chip on tool and hence friction between the chip and tool lowers [46, 47]. MQL is useful in providing lubrication but less efficient in removing heat from the vicinity of tool-workpiece interface. It increases the adhesion tendency of SiC particles that forms BUE on cutting edge [31]. This is also a reason for better results of R_a for cryogenic and CryoMQL machining in comparison with MQL machining. Hence, surface finish improved under cryogenic and CryoMQL machining. Specifically, lower values of R_a found for CryoMQL machining are owing to the combined impact of cryogenic fluid and lubrication at rake and flank face of cutting edge respectively.

As the value of v_c decreases at constant value of f, R_a increases for almost all cutting conditions. When the value of v_c is higher, cutting tool and workpiece are in direct contact for the lower time duration. It reduces the amount of BUE formed due to adhesion of hard SiC particles at cutting edge and hence lower surface roughness is formed [48]. The lower value of R_a observed in MQL technique at a lower value of v_c may be attributed to the reduction in diffusion wear. At

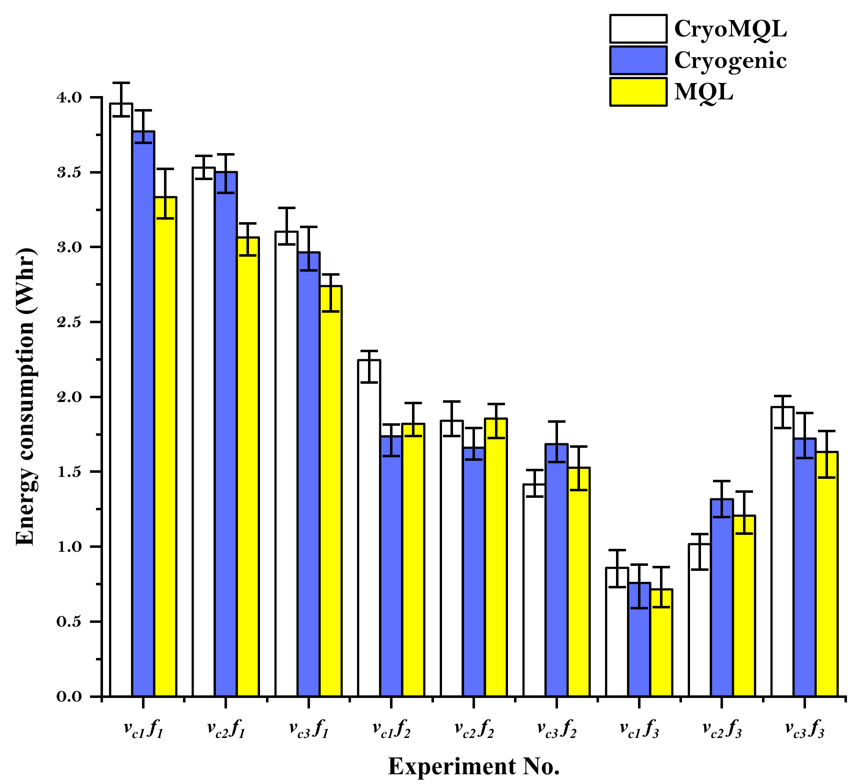

Fig. 10 Variation in energy consumption at different v_c and f under various cutting fluid strategies

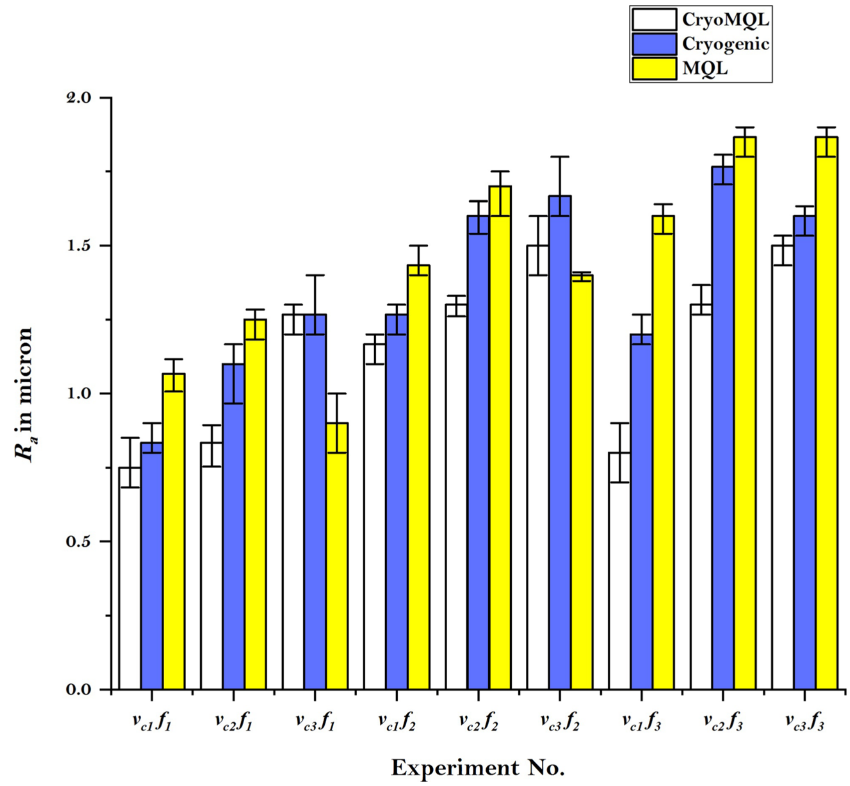

Fig. 11 Variation in R_a values at different v_c and f under various cutting fluid strategies

constant v_c, as the value of f raises, R_a increases for most of the combination of process parameters and cutting fluid strategies. It is attributed to the effect of feed marks on workpiece, as shown in Eq. 2 [49]. Besides, higher heat is generated with an increase in feed rate due to more plastic deformation at the primary shear zone. It increases cutting zone temperature and formation of the BUE which results in degraded surface quality [20].

$$R_a = \frac{f^2}{8r_\varepsilon} \tag{2}$$

Here f is longitudinal feed rate in mm/rev and r_ε is cutting tool nose radius in mm. At a combination of a higher value of v_c and f, the lowest value of R_a was observed under CryoMQL machining followed by cryogenic and MQL techniques in succession. This may be due to the fact that in CryoMQL machining, LN_2 and MQL are applied at rake and flank face of cutting tool, respectively. So, when the value of f increases, lesser time is available for cutting fluid to squeeze out from interface at tool-workpiece which reduces friction and decreases R_a as schematically shown in Fig. 13 [50].

3.4 Chip Breakability Analysis

Fang et al. [51] have developed a hybrid algorithm to predict chip breakability based on chip shape and its dimension. Pusavec et al. [52] used this algorithm to analyze chip breakability for machining of Inconel 718 alloy for different cooling and lubrication conditions. As per this algorithm, chip shapes are divided into four shapes viz. arc/bulky, circular/spiral, helical, and ribbon. Two major dimensional features are associated with each type of chip shape to analyze the CGM. Here the information obtained from CGM is used to calculate C_{in} as per Eq. 3. The values of C_{in} range from 0 to 1. For better chip breakability, a higher value of C_{in} is desirable.

$$c_{in} = \frac{\sum_{K=1}^{5}(\mu(A_k).\omega(A_k))}{\sum_{K=1}^{5}(\mu(A_k))} \tag{3}$$

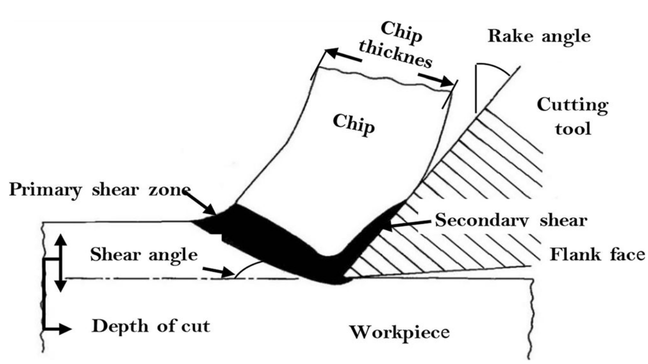

Fig. 12 A schematic of cutting process with chip formation and shear zone indication [41]

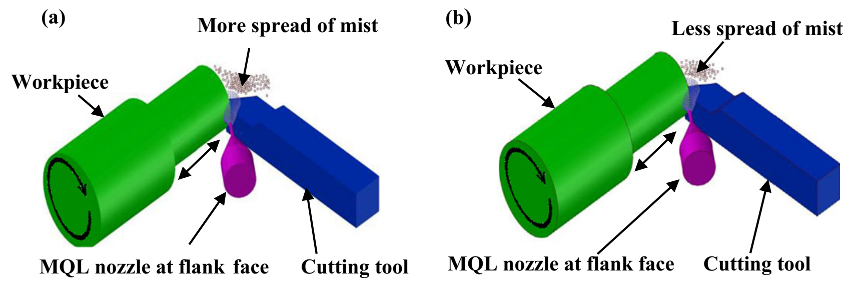

Fig. 13 A schematic of spread out of the mist in MQL machining at **(a)** higher feed rate and **(b)** lower feed rate

Here $\mu(A_k)$ represents chip form grade, which is calculated based on dimensional features. These dimensional features are then converted into linguistic variables by fuzzy logic. It forms a base to build CGM, which identifies the type of chips, namely VP (Very poor), P (Poor), F (Fair), G (Good), and E (Excellent). To quantify these intangible features, the value of $\omega(A_k)$ is assigned in the following manner. For the chip types VP, P, F, G, and E, value of $\omega(A_k)$ is designated as 0, 0.25, 0.50, 0.75 and 1, respectively. Figure 14 presents the photographs of different types of chips generated in this study. Table 7 presents the values of C_{in} for all turning tests under three cutting fluid strategies.

From Table 7, it can be observed that for MQL, cryogenic and CryoMQL processes the value of C_{in} is higher for v_c of 62 m/min and all levels of f except at higher level of f for CryoMQL machining. The lower value of C_{in} for CryoMQL machining may be due to lesser friction at tool-workpiece contact, which promotes a continuous type of chips. When the value of v_c is 27 m/min, MQL machining outperformed CryoMQL and cryogenic machining based on C_{in} at most of the values of f.

In cryogenic machining, at higher values of v_c and f, the C_{in} outperformed other cutting fluid strategies owing to embrittlement of chips at cryogenic temperature, which makes it easy to break chips [49]. For all combinations of cutting parameters with different cooling and lubrication techniques, segmented type of chips are produced which indicate the loss of ductility because of the existence of hard SiC particles [18, 22].

4 Conclusions

In this study, environmentally-friendly cutting conditions, namely MQL, cryogenic, and CryoMQL machining, have been analyzed based on cutting force, energy consumption, R_a and C_{in}, when in-house developed AZ91/5SiC PMMCs is turned. In this study, an intensive approach is followed to optimize MQL parameters. Based on the above discussion following conclusions may be drawn.

- It has been observed that MQL parameters namely standoff distance, nozzle angle and flow rate of oil significantly influence the quality of droplets generated during MQL. The 30 mm standoff distance, 75° nozzle angle and 14 ml/h are found out as optimum MQL parameters.
- The 40.39% and 64.65%; 7.13% and 11.49% higher value of cutting force and energy consumption is found correspondingly for CryoMQL and cryogenic machining respectively in comparison with MQL technique by considering the mean of all turning tests. The 25.59% and 18.35% lower values of R_a have been observed in case of CryoMQL machining considering all turning tests, as compared to MQL and cryogenic machining respectively. The increment in hardness of workpiece material are responsible for generating higher cutting force and energy consumption in cryogenic and CryoMQL techniques. The lower values of R_a observed in MQL machining is due to adhesion of SiC particles on cutting tool.

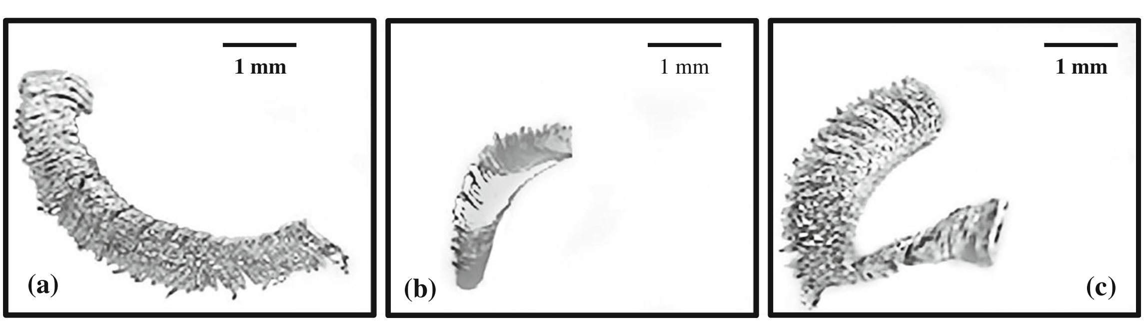

Fig. 14 Photographs of chip type **(a)** circular **(b)** arc/bulky **(c)** ribbon

Table 7 Values of C_{in} for CryoMQL, cryogenic and MQL machining

Test No.	v_c (m/min)	*f* (mm/rev)	*C_{in} for CryoMQL*	*Chip type (Cryo MQL)*	*C_{in} for Cryogenic*	*Chip Type (Cryogenic)*	*C_{in} for MQL*	*Chip type (MQL)*
1	62	0.111	1	Arc / Bulky	1	Arc /Bulky	1	Arc /Bulky
2	41	0.111	0.95	Arc / Bulky	0.92	Circular	1	Arc /Bulky
3	27	0.111	1	Circular	0.8	Arc /Bulky	0.83	Circular
4	62	0.222	1	Arc / Bulky	1	Arc /Bulky	1	Arc /Bulky
5	41	0.222	1	Arc / Bulky	1	Arc /Bulky	1	Arc /Bulky
6	27	0.222	0.75	Ribbon	0.75	Ribbon	1	Arc /Bulky
7	62	0.333	0.75	Ribbon	1	Arc /Bulky	0.93	Arc /Bulky
8	41	0.333	1	Arc / Bulky	1	Arc /Bulky	0.8	Circular
9	27	0.333	0.67	Ribbon	0.75	Ribbon	1	Arc /Bulky

- Segmented type of chips is found for all cooling and lubrication techniques. The comparable values of chip breakability index are observed for CryoMQL, cryogenic and MQL machining. However, higher value of C_{in} is found for LN_2 as cutting fluid in comparison with MQL and CryoMQL machining at $v_{c1}f_3$.

This study elucidates a thorough approach to optimize MQL parameters experimentally. To provide a sustainable solution of carbon-based conventional flood machining, MQL, cryogenic and CryoMQL machining setups have been developed. Cryogenic and CryoMQL machining techniques are found to be superior in terms of surface roughness and chip breakability index while lower cutting force and energy consumption are found in MQL machining.

Acknowledgments This research has been conducted under the project titled "Design and Development of Energy Efficient Cryogenic Machining Facility for Heat Resistant Alloys and Carbon Fibre Composite". It is funded by the Government of India, code of fund SERB-DST, Project code ECR/2016/000735.

References

1. Bayraktar Ş, Afyon F (2020) Machinability properties of Al–7Si, Al–7Si–4Zn and Al–7Si–4Zn–3Cu alloys. J Braz Soc Mech Sci Eng 42:187
2. Balamurugan K, Uthayakumar M, Thirumalai Kumaran S, Samy GS, Pillai UTS (2019) Drilling study on lightweight structural mg/SiC composite for defence applications. Defence Technol 15(4): 557–564
3. Pramanik A, Zhang LC (2017) Particle fracture and debonding during orthogonal machining of metal matrix composites. Adv Manuf 5(1):77–82
4. Tamizharasan T, Senthilkumar N, Selvakumar V, Dinesh S (2019) Taguchi's methodology of optimizing turning parameters over chip thickness ratio in machining P/M AMMC. SN Appl Sci 1:160
5. Bayraktar Ş, Demir O (2020) Processing of T6 heat-treated Al-12Si-0.6Mg alloy. Mater Manuf Process 35:354–362
6. Balamurugan K, Uthayakumar M, Ramakrishna M, Ramakrishna M, Pillai UTS (2020) Air jet Erosion studies on mg/SiC composite. Silicon 12:413–423
7. Yap TC, El-Tayeb NSM, von Brevern P (2013) Cutting forces, friction coefficient and surface roughness in machining Ti-5Al-4V-0.6Mo-0.4Fe using carbide tool K313 under low pressure liquid nitrogen. J Braz Soc Mech Sci Eng 35:11–15
8. Adler DP, Hii WS, Michalek DJ, Sutherland JW (2006) Examining the role of cutting fluids in machining and efforts to address associated environmental/health concerns. Mach Sci Technol 10(1):23–58
9. Rahim EA, Sasahara H (2011) A study of the effect of palm oil as MQL lubricant on high speed drilling of titanium alloys. Tribol Int 44(3):309–317
10. Khanna N, Pusavec F, Agrawal C, Krolczyk GM (2020) Measurement and evaluation of hole attributes for drilling CFRP composites using an indigenously developed cryogenic machining facility. Measurement 154:107504
11. Shah P, Chetan KN (2020) Comprehensive machining analysis to establish cryogenic LN_2 and LCO_2 as sustainable cooling and lubrication techniques. Tribol Int 148:106314
12. Khanna N, Agrawal C, Gupta MK, Song Q, Singla AK (2020) Sustainability and machinability improvement of Nimonic-90 using indigenously developed green hybrid machining technology. J Clean Prod 263:121402
13. Shah P, Khanna N, Zadafiya K, Bhalodiya M, Maruda RW, Krolczyk GM (2020) In-house development of eco-friendly lubrication techniques (EMQL, Nanoparticles+EMQL and EL) for improving machining performance of 15–5 PHSS. Tribol Int 151: 106476
14. Setti D, Sinha MK, Ghosh S, Rao PV (2014) An effective method to determine the optimum parameters for minimum quantity lubrication (MQL) grinding. 5th Int 26th all India Manuf techno des res Conf IIT Guwahati Assam India 67
15. Thakur A, Manna A, Samir S (2020) Multi-response optimization of turning parameters during machining of EN-24 steel with SiC Nanofluids based minimum quantity lubrication. Silicon 12:71–85
16. Bayraktar Ş (2020) In: high speed machining, Gupta K, Davim JP(ed) cryogenic cooling-based sustainable machining, Elsevier-academic press, London, Chapter-8, pp. 223-241
17. Sivaiah P, Chakradhar D (2019) The effectiveness of a novel cryogenic cooling approach on turning performance characteristics during machining of 17-4 PH stainless steel material. Silicon 11:25–38
18. Shokrani A, Dhokia V, Newman ST (2018) Energy conscious cryogenic machining of Ti-6Al-4V titanium alloy. Proc Inst Mech Eng Part B J Eng Manuf 232(10):1690–1706

19. Khann N, Suri NM, Shah P, Hegab H, Mia M (2020) Cryogenic turning of in-house cast magnesium based MMCs : a comprehensive investigation. J Mater Res Technol 9:7628–7643
20. Yin W, Duan C, Sun W, Wei B (2020) Analytical model of cutting temperature for workpiece surface layer during orthogonal cutting particle reinforced metal matrix composites. J Mater Process Technol 282:116643
21. Soorya Prakash K, Gopal PM, Karthik S (2020) Multi-objective optimization using Taguchi based grey relational analysis in turning of rock dust reinforced aluminum MMC. Measurement 157: 107664
22. Khanna N, Suri NM, Agrawal C, Shah P, Krolczyk GM (2019) Effect of Hybrid Machining Techniques on Machining Performance of In-House Developed Mg-PMMC. Trans Ind Inst Met 72:1799–1807
23. Outeiro JC, Rossi F, Fromentin G, Poulachon G, Germain G, Batista AC (2013) Process mechanics and surface integrity induced by dry and cryogenic machining of AZ31B-O magnesium alloy. Procedia CIRP 8:487–492
24. Bai W, Roy A, Sun R, Silberschmidt VV (2019) Enhanced machinability of SiC-reinforced metal-matrix composite with hybrid turning. J Mater Process Technol 268:149–161
25. Dinesh S, Senthilkumar V, Asokan P (2017) Experimental studies on the cryogenic machining of biodegradable ZK60 mg alloy using micro-textured tools. Mater Manuf Process 32(9):979–987
26. Zou L, Huang Y, Zhou M, Yang Y (2018) Effect of cryogenic minimum quantity lubrication on machinability of diamond tool in ultraprecision turning of 3Cr2NiMo steel. Mater Manuf Process 33(9):943–949
27. Sartori S, Ghiotti A, Bruschi S (2017) Hybrid lubricating/cooling strategies to reduce the tool wear in finishing turning of difficult-to-cut alloys. Wear 376:107–114
28. Sales WF, Diniz AE, Machado ÁR (2001) Application of cutting fluids in machining processes. J Braz Soc Mech Sci Eng 23(2):227–240
29. Pereira O, Rodríguez A, Fernández-Abia AI, Barreiro J, de Lacalle LL (2016) Cryogenic and minimum quantity lubrication for an eco-efficiency turning of AISI 304. J Clean Prod 13(9):440–449
30. Yildirim ÇV, Kivak T, Sarikaya M, Şirin Ş (2019) Evaluation of tool wear, surface roughness/topography and chip morphology when machining of Ni-based alloy 625 under MQL, cryogenic cooling and CryoMQL. J Mater Res Technol 9(2):2079–2092
31. Karabulut Ş, Gökmen U, Çinici H (2016) Study on the mechanical and drilling properties of AA7039 composites reinforced with $Al_2O_3/B_4C/SiC$ particles. Compos Part B Eng 93:43–55
32. Bhowmick S, Lukitsch MJ, Alpas AT (2010) Dry and minimum quantity lubrication drilling of cast magnesium alloy (AM60). Int J Mach Tools Manuf 50(5):444–457
33. Suda S, Yokota H, Inasaki I, Wakabayashi T (2002) A synthetic Ester as an optimal cutting fluid for minimal quantity lubrication machining. CIRP Ann - Manuf Technol 51(1):95–98
34. Khanna N, Agrawal C, Joshi V (2017) Zero Vapor Loss Integrated Cryogen Phase Separator Indian patents 2017201721031291 a
35. Khanna N, Davim JP (2015) Design-of-experiments application in machining titanium alloys for aerospace structural components. Measurement 61:280–290
36. Bhowmick S, Alpas AT (2011) The role of diamond-like carbon coated drills on minimum quantity lubrication drilling of magnesium alloys. Surf Coat Technol 205(23–24):5302–5311
37. Kaynak Y (2014) Evaluation of machining performance in cryogenic machining of Inconel 718 and comparison with dry and MQL machining. Int J Adv Manuf Technol 72(5–8):919–933
38. Bilga PS, Singh S, Kumar R (2016) Optimization of energy consumption response parameters for turning operation using Taguchi method. J Clean Prod 137:1406–1417
39. Frantsen JE, Mathiesen T (2009) Specifying stainless steel surface for the brewery, dairy and pharmaceutical sectors. In proceedings of the corrosion 2009, Atlanta, GA, USA, 22–26 march 2009
40. Rowe GW, Smart F (1966) Vapour lubrication in friction and low-speed metal cutting. Pro Inst Mech Eng Conf Proc Paper 23 181(15):48–57
41. Wakabayashi T, Williams JA, Hutchings IM (1993) The action of gaseous lubricants in the orthogonal machining of an Aluminium alloy by titanium nitride coated tools. Surf Coat Technol 57:183–189
42. Wakabayashi T, Inasaki I, Suda S (2006) Tribological action and optimal performance: research activities regarding Mql machining fluids. Mach Sci Technol 10(1):59–85
43. Nicholls CJ, Boswell B, Davies IJ, Islam MN (2016) Review of machining metal matrix composites. Int J Adv Manuf Technol 90: 2429–2441
44. Arulkirubakaran D, Balasubramanian K, Raju R, Palanisamy D, Manikandan N (2019) Machinability studies on precipitation hardened stainless steel using Cryo-treated textured carbide inserts. Mater Manuf Process 78:216–222
45. Yildiz Y, Nalbant M (2008) A review of cryogenic cooling in machining processes. Int J Mach Tools Manuf 48(9):947–964
46. Hong SY, Ding Y, Jeong W (2001) Friction and cutting forces in cryogenic machining of Ti-6Al-4V. Int. J. Mach. Tools Manuf 41: 2271–2285s
47. Khanna N, Agrawal C, Gupta MK, Song Q (2019) Tool wear and hole quality evaluation in cryogenic Drilling of Inconel 718 superalloy. Tribol Int 143:106084
48. Karabulut Ş (2015) Optimization of surface roughness and cutting force during AA7039/Al_2O_3 metal matrix composites milling using neural networks and Taguchi method. Measurement 66:139–149
49. Khanna N, Shah P, Agrawal C, Pusavec F, Hegab H (2020) Inconel 718 machining performance evaluation using indigenously developed hybrid machining facilities: experimental investigation and sustainability assessment. Int J Adv Manuf Technol 106:4987–4999
50. Persson B N (2013) Sliding friction: physical principles and applications. Springer Science and Business Media Heidelberg
51. Fang XD, Fei J, Jawahir IS (1996) A hybrid algorithm for predicting chip form/chip breakability in machining. Int J Mach Tools Manuf 36(10):1093–1107
52. Pusavec F, Deshpande A, Yang S, M'Saoubi R, Kopac J, Dillon Jr OW, Jawahir IS (2015) Sustainable machining of high temperature nickel alloy–Inconel 718: part 2–chip breakability and optimization. J Clean Prod 87:941–952